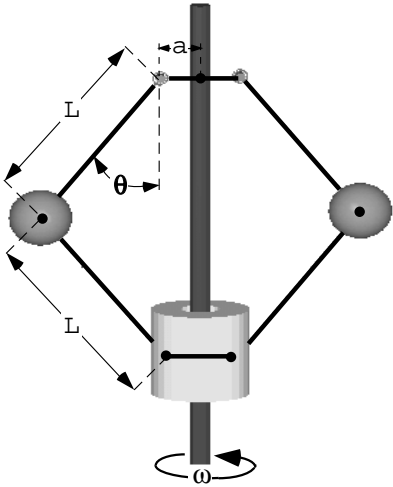
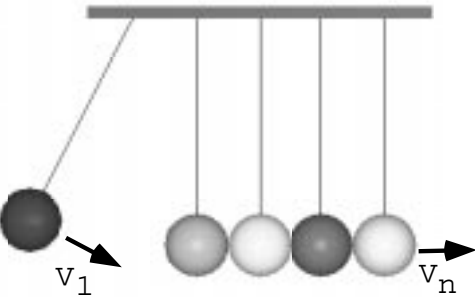
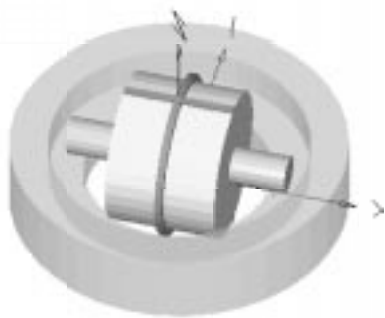
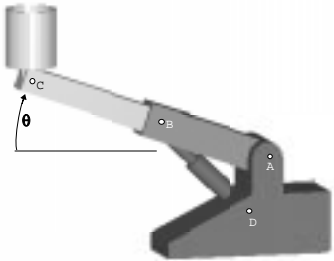
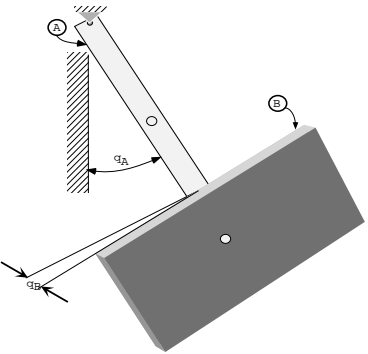
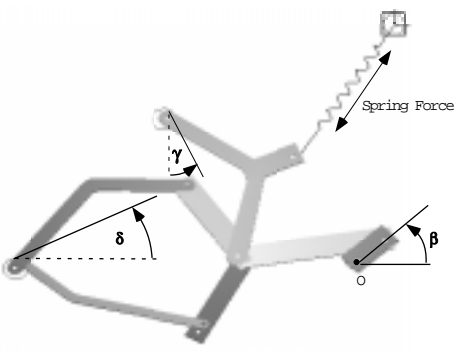
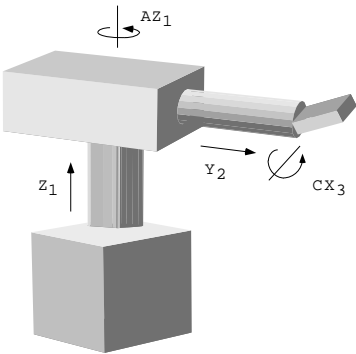


Demonstration and Validation of Visual Nastran Motion



Abstract

This document serves two purposes. First, it validates various aspects of VISUAL NASTRAN including kinematics, kinetics, dynamics, contact, and collisions. Detailed example problems demonstrating these key phenomena are given and comparisons of their VISUAL NASTRAN results to closed-form solutions, numerical solutions from textbooks and published technical papers, and numerical solutions obtained from other multi-body codes, e.g., AUTOLEV, DADS, and ADAMS are presented. By perusing this report and by comparing VISUAL NASTRAN with other motion simulation packages, it should be clear what VISUAL NASTRAN offers in contrast to your current motion simulation tools.

Secondly, this document demonstrates the extensive motion simulation capabilities of VISUAL NASTRAN through the study of several interesting mechanical systems. These mechanical systems were chosen because they are educational, physically demonstratable, and although relatively simple, exhibit surprisingly complex motions. It is hoped that some “intuition” for three dimensional motion may be gleaned from these instructive examples.

Contents

Abstract	2
1 Benchmarks: Comparison with other numerical packages	4
1.1 Serial Mechanism: Robot	4
1.2 Closed-chain Mechanism: Seven Bar Linkage	6
2 Textbook Problems	8
2.1 Chaotic Systems: The Babyboot	8
2.2 Stability Analysis: Torque-free Motions of a Rigid Body	10
2.3 Centrifugal Forces: The Governor	12
2.4 Static Constraint Forces: The Telescoping Arm	13
2.5 Collisions: Newton's Cradle	14

Chapter 1

Benchmarks: Comparison with other numerical packages

1.1 Serial Mechanism: Robot

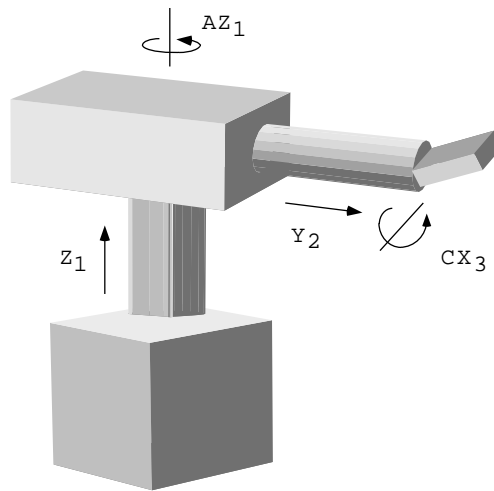


Figure 1.1: Serial Robot from Multibody Systems Handbook

Fig. 1.1 is a schematic representation of a serial robot. This mechanism is important because it served as one of two benchmark test cases in a recent multibody systems handbook [18]. The contributors to this handbook include many of the manufacturers of dynamic analysis software, e.g., Mechanical Dynamics (ADAMS), CADSI (DADS), and OnLine Dynamics (AUTOLEV).

The robot consists of three bodies: the robot base, a robot arm, and a robot hand. The motion of the robot is controlled by four motors/actuators which lift and rotate the robot arm while extending and rotating the robot hand. A complete description of the system, including its joints, mass and inertia properties, and initial values is found in [18, pp. 16-18]. A VISUAL NASTRAN file named *SerialRobot.wm3* is distributed in the *Validate* directory of the VISUAL NASTRAN CD.

1.1.1 Results

The simulation results obtained from VISUAL NASTRAN are shown in Figures (1.2-1.5). These graphs match those generated by DADS [18, pp. 179] and ADAMS [18, pp. 395]. Numerical results from VISUAL NASTRAN can be compared to numerical results obtained for the robot hand's global position from AUTOLEV [18, pp. 102] at the end of the simulation ($t=2.0$ sec). From the table below, it is evident that VISUAL NASTRAN can produce results which are accurate to one part in a million.

VISUAL NASTRAN	x=2.9285459	y=3.209857	z=4.414592
AUTOLEV	x=2.9285436	y=3.209855	z=4.414599

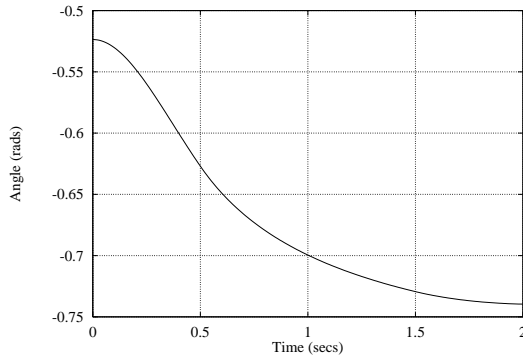


Figure 1.2: Rotation of Robot Base (AZ_1)

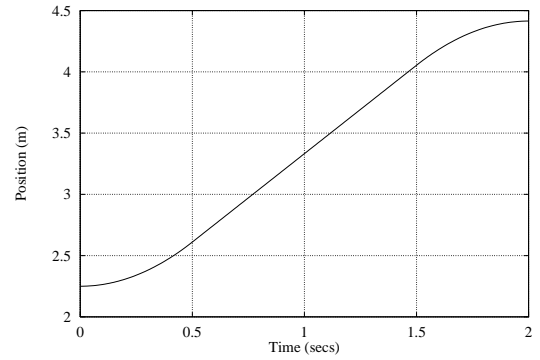


Figure 1.3: Elevation of Robot Arm (Z_1)

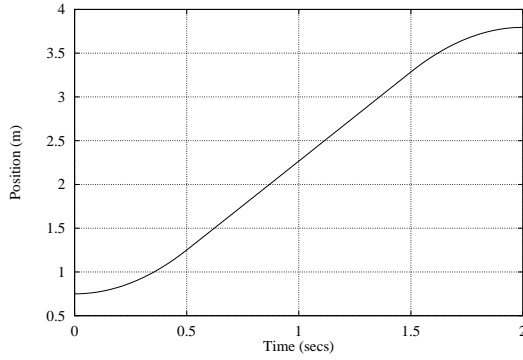


Figure 1.4: Extension of Robot Arm (Y_2)

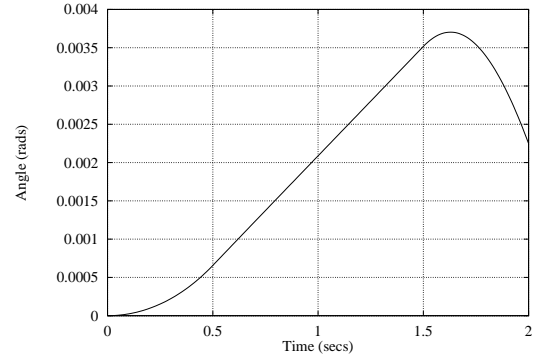


Figure 1.5: Rotation of Robot Hand (CX_3)

1.2 Closed-chain Mechanism: Seven Bar Linkage

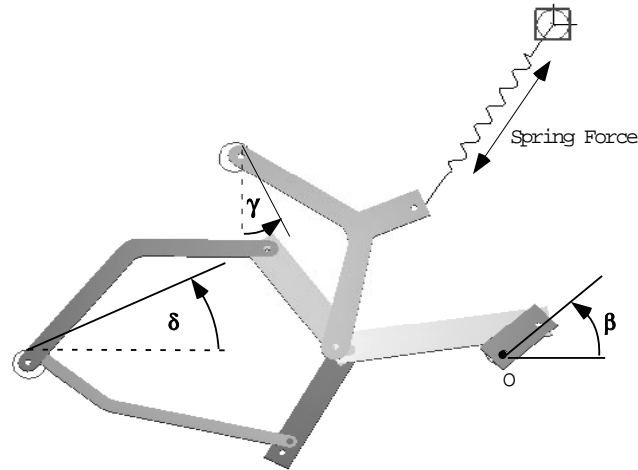


Figure 1.6: Closed-chain Mechanism from Multibody Systems Handbook

Fig. 1.6 is a schematic representation of a closed-chain mechanism. This mechanism is important because it served as one of two benchmark test cases in a recent multibody systems handbook [18]. The contributors to this handbook include many of the manufacturers of dynamic analysis software, e.g., Mechanical Dynamics (ADAMS), CADSI (DADS), and OnLine Dynamics (AUTOLEV).

The mechanism consists of seven bodies interconnected by frictionless revolute joints. This one degree of freedom mechanism is driven by a constant-torque motor located at point O . A complete description of the system, including its joints, mass and inertia properties, and initial values is found in [18, pp. 10-15]. A VISUAL NASTRAN file named *ClosedLoop.wm3* is distributed in the *Validate* directory of the VISUAL NASTRAN CD.

1.2.1 Results

The simulation results obtained from VISUAL NASTRAN are shown in Figures (1.7-1.10). These graphs match those generated by ADAMS [18, pp. 394]. DADS did *not* produce results for this problem. Numerical results from VISUAL NASTRAN can be compared to numerical results obtained for β , γ , and δ , from AUTOLEV [18, pp. 99] after several revolutions ($t=0.03$ sec). From the table below, it is evident that VISUAL NASTRAN produces results accurate to three significant digits, the same accuracy given in the initial values in [18]. One interesting note is that the ADAMS simulation was reported to require *182 equations* and *380 CPU seconds* on a Vaxstation 2000. VISUAL NASTRAN required only *35 equations*, *20 seconds* of calculation time, and *21 seconds* of display time on a 266 Mhz Pentium PC.

VISUAL NASTRAN	$\gamma=0.0407$ rad	$\beta=15.81$ rad	$\delta=0.5244$ rad
AUTOLEV	$\gamma=0.0409$ rad	$\beta=15.81$ rad	$\delta=0.5247$ rad

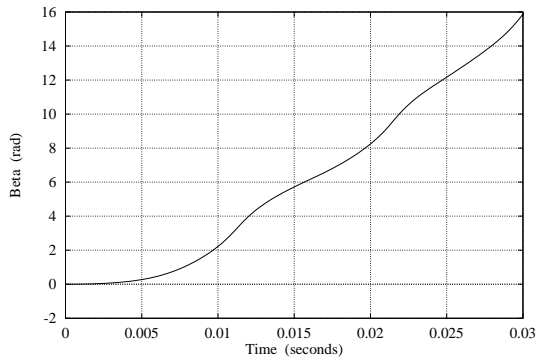


Figure 1.7: Time History of β

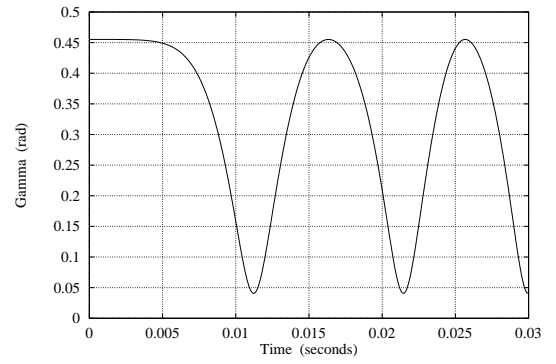


Figure 1.8: Time History of γ

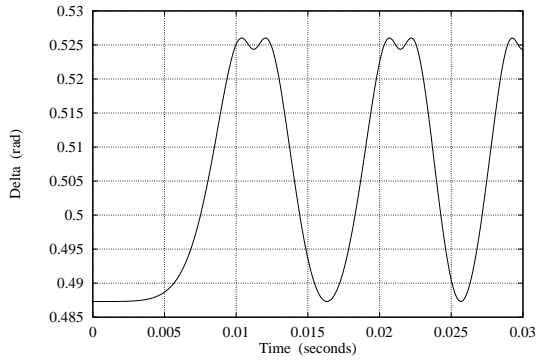


Figure 1.9: Time History of δ

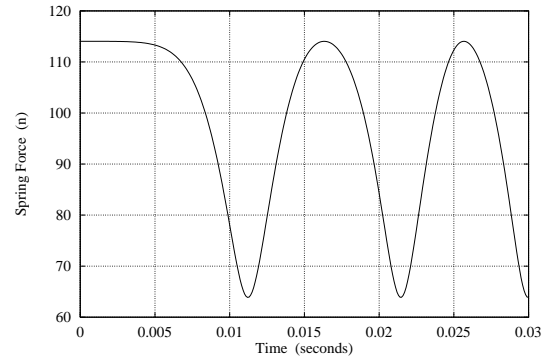


Figure 1.10: Magnitude of Spring Force

Chapter 2

Textbook Problems

2.1 Chaotic Systems: The Babyboot

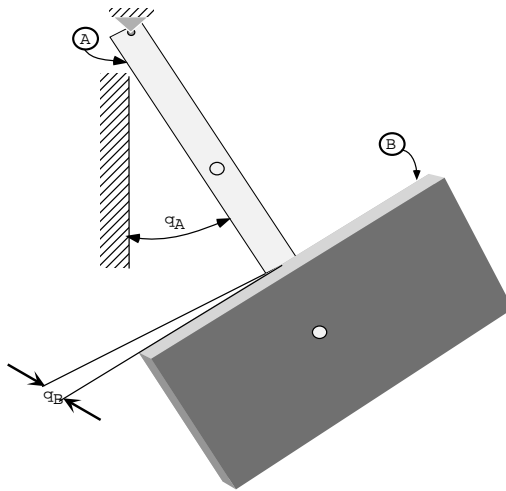


Figure 2.1: Babyboot Schematic

Fig. 2.1 is a schematic representation of a swinging babyboot attached by a shoelace to a rigid support. This problem first appeared in [9]. This simple system is interesting because at times, its motion is “chaotic”, meaning that small perturbations in initial values or inaccuracies in numerical integration lead to dramatically different results. In order to produce simulations, one must formulate equations of motion and numerically integrate the resulting dynamical differential equations. The results of this problem were compared with numerical result from [10, pp. 339-340]

The modeling of the system in Fig. 2.1 is done with a thin uniform rod A and a uniform plate B. The rod A is attached to a fixed support by a revolute joint and B is connected to A at the mass center of B in such a way that B can rotate freely about the axis of A. (Note: the revolute joints’ axes are perpendicular *not* parallel.) The quantities q_A and q_B denote angles associated with the rotation of A and B, respectively. A complete description of the system, including its joints, mass and inertia properties, and initial values is found in [10, pp. 329-330, 339-340]. A VISUAL NASTRAN file named *babyboot.wm3*

is distributed in the *Validate* directory of the VISUAL NASTRAN CD.

2.1.1 Results

The simulation results obtained from VISUAL NASTRAN are shown in Figures (2.2-2.3). These graphs match those found in [10, pp. 339-340]. In order to produce Fig. 2.2, $q_A(0)$ was set to 45° and $q_B(0)$ was set to either 0.5° or 1.0° . As can be seen, q_B is stable, meaning that as $q_B(0)$ is made sufficiently small, $q_B(t)$ can be made arbitrarily small. Although q_B is stable for small values of $q_A(0)$, larger values of $q_A(0)$ cause instability in q_B . This fact is evident from Fig. 2.3 which shows that q_B is *very* sensitive to initial values. A 0.5° change in the value of $q_B(0)$ results in a 2000° difference in the value of $q_B(10)$! This sensitivity also manifests itself in other ways. Loose numerical integration tolerances or nearly *any* numerical inaccuracies produce vastly different results than the ones shown in Fig. 2.3. Because of this fact, this relatively simple problem serves as a good test problem for VISUAL NASTRAN. Another non-intuitive phenomenon of this problem is that increasing $q_A(0)$ further to 135° restabilizes q_B , but as $q_A(0)$ gets close to 180° , it destabilizes q_B once more.

Numerical results from VISUAL NASTRAN can be compared to numerical results obtained for q_A and q_B at $t=10.0$ sec for a simulation with initial values of $q_A(0) = 90^\circ$ and $q_B(0) = 1^\circ$. From the table below, it is clear that VISUAL NASTRAN produces accurate results.

VISUAL NASTRAN	$q_A = -61.17^\circ$	$q_B = -928.347^\circ$
Kane and Levinson	$q_A = -61.313^\circ$	$q_B = -929.478^\circ$

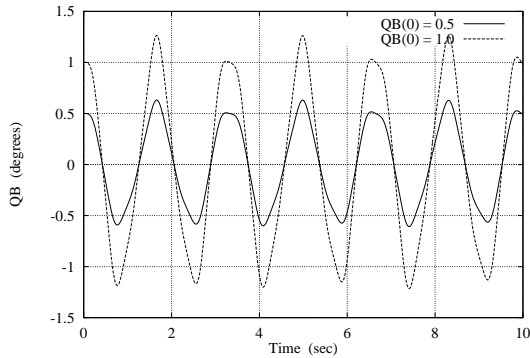


Figure 2.2: $q_B(t)$ with $q_A(0) = 45^\circ$

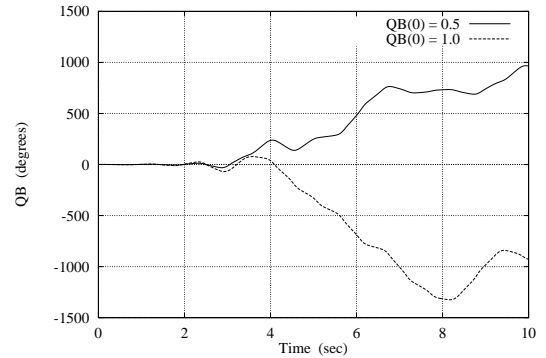


Figure 2.3: $q_B(t)$ with $q_A(0) = 90^\circ$

2.2 Stability Analysis: Torque-free Motions of a Rigid Body

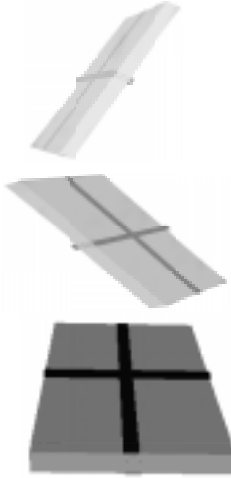


Figure 2.4: Spinning Book

The equations which govern the rotational motions of a single rigid body pose an analytical challenge because they are nonlinear and possess closed form solutions only in a few special cases. This fact highlights one of the many difficulties in performing 3D motion simulations. In this section, the rotational motion of a torque-free rigid body is examined and compared with a closed form solution in [6, pp. 96-124]. The closed form solution is not presented here because it is fairly complicated and involves Jacobi elliptic functions. A complete description of this system can be ascertained from the VISUAL NASTRAN file named *BookSpin.wm3*, which is distributed in the *Validate* directory of the VISUAL NASTRAN CD.

The pertinent features of the rigid body B under consideration are that B has central principal moments of inertia I_1, I_2, I_3 where $I_1 \leq I_2 \leq I_3$ and B is rotating with an inertial angular velocity $\omega_1 \mathbf{b}_1 + \omega_2 \mathbf{b}_2 + \omega_3 \mathbf{b}_3$. The unit vectors $\mathbf{b}_1, \mathbf{b}_2$, and \mathbf{b}_3 are fixed in B and parallel to the central principal axes of B. After choosing numerical values of 416 kg m^2 , 916 kg m^2 , and 1300 kg m^2 , for I_1, I_2 , and I_3 , respectively, three cases were simulated for 10 secs with an integration step of 0.02 secs and an absolute error tolerance of $1.0e^{-5}$. The initial values for each of the cases are given below.

Case	$\omega_1(0)$ rad/sec	$\omega_2(0)$ rad/sec	$\omega_3(0)$ rad/sec
1	5	0	0.05
2	0.05	5	0
3	0	0.05	5

Case 1 represents a perturbation of a simple spin about \mathbf{b}_1 , the *minimum* principal axis. Spin about the minimum principal axis is said to be *stable* in the Liapunov sense. This is evident from the animation in *BookSpin.wm3* and from Figure 2.5 which displays the minor variation in the values γ , the angle¹ between the (fixed) angular momentum vector \mathbf{h} and \mathbf{b}_1 .

Case 2 is a perturbation of a simple spin about \mathbf{b}_2 , the *intermediate* principal axis. Spin about the

¹In classical mechanics literature, γ is called the *nutaton* angle

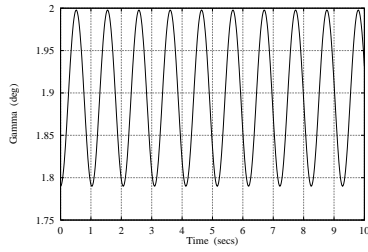


Figure 2.5: γ -Minor Axis

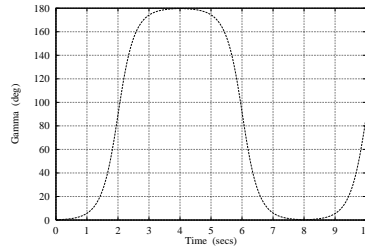


Figure 2.6: γ -Intermediate Axis

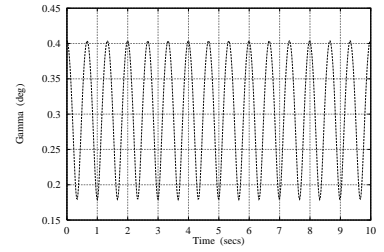


Figure 2.7: γ -Major Axis

intermediate axis is *unstable*. This is evident from the animation in *BookSpin.wm3* and from Figure 2.6 which shows the dramatic variation in the values of the angle between \mathbf{h} and \mathbf{b}_2 .

Lastly, Case 3 is a perturbation of a simple spin about \mathbf{b}_3 , the *maximum* principal axis. Spin about the maximum axis is *stable*. This is shown in the animation in *BookSpin.wm3* and in Figure 2.6 which displays the minor variation in the values of the angle between \mathbf{h} and \mathbf{b}_3 .

The accuracy of VISUAL NASTRAN results can be determined from a variety of tests. One test is the ability of VISUAL NASTRAN to maintain the constancy of kinetic energy and the magnitude of angular momentum, two quantities which are theoretical conserved during the simulation. A second test is the error in ω_1 , ω_2 , and ω_3 at 10 secs. From the table below, the accuracy of VISUAL NASTRAN can be inferred.

Case	Maximum Error in Energy (joules)	Maximum Error in Angular Momentum	Error in $\omega_1(10)$ rad/sec	Error in $\omega_2(10)$ rad/sec	Error in $\omega_3(10)$ rad/sec
1	$6.0e^{-12}$	$1.2e^{-12}$	$3.5e^{-10}$	$2.7e^{-8}$	$2.4e^{-8}$
2	$6.3e^{-8}$	$1.2e^{-8}$	$2.6e^{-7}$	$2.4e^{-6}$	$1.7e^{-7}$
3	$1.8e^{-11}$	$3.6e^{-12}$	$2.6e^{-7}$	$1.8e^{-8}$	$7.1e^{-11}$

2.3 Centrifugal Forces: The Governor

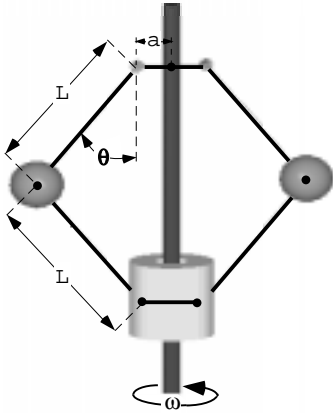


Figure 2.8: Centrifugal Governor

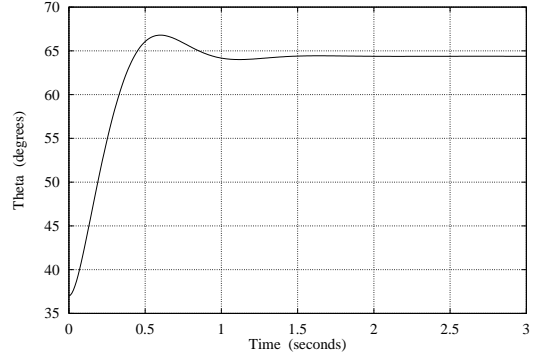


Figure 2.9: Convergence of θ on exact result

The equations which govern the configuration of a device undergoing *steady* motion are not readily solved by most multibody numerical codes. However, the steady state configuration of the system may be determined by simulating the *full* nonlinear motion and adding damping to the system so that it ultimately settles to the desired configuration. In this section, the steady motion of a centrifugal governor is examined and compared with a closed form solution in [5, pp. 193-194]. A complete description of this system can be ascertained from the VISUAL NASTRAN file named *Governor.wm3*, which is distributed in the *Validate* directory of the VISUAL NASTRAN CD.

The flyball engine governor depicted in Figure 2.8 consists of two uniform spheres S of mass m^S and a third heavier particle P of mass m^P linked together by light hinged bars of length L as shown. The particle P can slide freely on a vertical shaft, which spins at a uniform angular speed ω . Due to centrifugal forces on the spheres, P can be lifted so that θ , the angle between the local vertical and one of the light bars, depends on ω . According to [5, pp. 193-194], the value of θ is governed by the nonlinear algebraic equation

$$\frac{\tan \theta}{\sin \theta + a/l} = \omega^2 \frac{m^S l}{(m^S + m^P)g} \quad (2.1)$$

Substituting the values $\omega=1200$ deg/sec, $m^S=2.0$ kg, $m^P=10$ kg, $L=0.254$ m, $a=0.0508$ m, and $g=9.81$ m/sec², into equation (2.1) produces

$$\frac{\tan \theta}{\sin \theta + 0.2} = 1.89291314069 \quad (2.2)$$

Equation (2.2) can be solved with a multitude of methods including trial and error and graphical methods as well as the method of bisection, secant, Brent, Ridder, or Newton-Rhapson. The numerical solution of equation (2.2) is $\theta=64.381201^\circ$. With VISUAL NASTRAN, one does not have to deal with solving difficult nonlinear equations, instead it is only necessary to add damping and run the simulation until θ converges to its quasi-static value. After 3 seconds, the VISUAL NASTRAN value for θ is 64.38123205° within $3.2e^{-5}$ of the exact result. Figure 2.9 demonstrates the convergence of θ to its theoretical value.

2.4 Static Constraint Forces: The Telescoping Arm

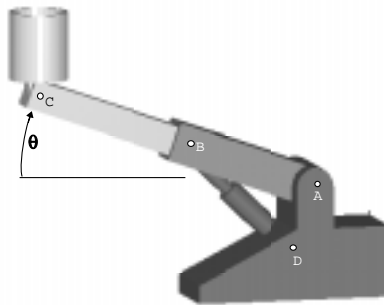


Figure 2.10: Telescoping Arm Schematic

Fig. 2.10 is a schematic representation of a telescoping arm used to elevate a platform for construction and utilities workers. The system consists of light bucket C carrying men and equipment of weight 500 lbs, a light telescoping arm ABC , and a piston between B and D which controls the angle θ between the horizontal and ABC . This system was chosen to validate static solutions produced by VISUAL NASTRAN, and the results of this problem were compared with a closed form solution from [1, pg. 557]. A VISUAL NASTRAN file named *telescop.wm3* is distributed in the *Validate* directory of the VISUAL NASTRAN CD.

2.4.1 Results

The magnitude of the force exerted by the piston on the telescoping arm as a function of θ is shown in Figure 2.11. The values found in this graph match those produced by AUTOLEV and exactly match those found in [1, pg. 557] when $\theta=20^\circ$. The information in Figure 2.11 is useful for sizing the piston's hydraulic motor.

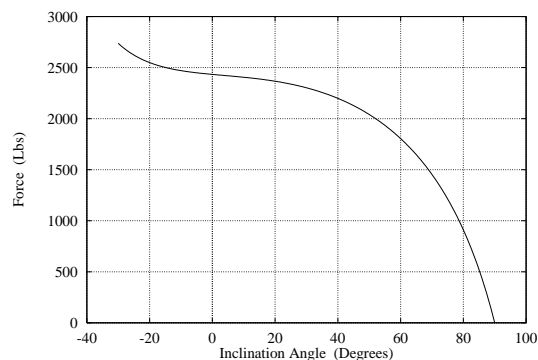


Figure 2.11: Magnitude of piston force vs. θ

2.5 Collisions: Newton's Cradle

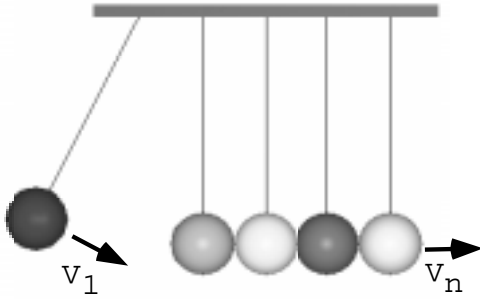


Figure 2.12: Newton's Cradle1

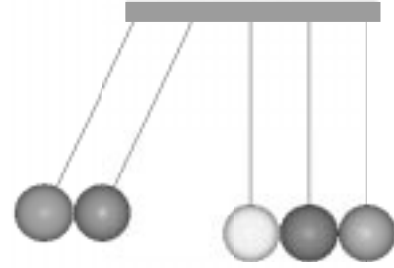


Figure 2.13: Newton's Cradle2

Fig. 2.12 is a schematic representation of an executive desk toy, sometimes called a “Newton's Cradle”. This system was chosen to validate collision solutions produced by VISUAL NASTRAN. The VISUAL NASTRAN results of this problem, available in the *NewtonCradle.wm3* file, were compared with a closed form solution in [11, pp. 206-207]. VISUAL NASTRAN uses impulse-momentum theory and a coefficient of restitution in predicting collision responses.²

The system in Fig. 2.12 consists of five homogenous spheres of equal mass m suspended by parallel wires of equal length L so that the spheres are touching each other. The first sphere is released so that it strikes the second sphere with a speed v_1 . The coefficient of restitution between all the spheres is e .

2.5.1 Results

When the first sphere strikes the second, which subsequently strikes the third, etc., the center of mass of the n^{th} sphere is theoretically imparted a velocity of magnitude $v_n = v_1 \left(\frac{1+e}{2}\right)^{n-1}$. The following table compares the theoretical results for v_5 with those obtained for VISUAL NASTRAN for various values of e .³

Coefficient of restitution	Theoretical solution	Visual Nastran solution	Difference
1.0	0.7880776	0.7881982	$1.2e^{-4}$
0.75	0.4620277	0.4619566	$7.1e^{-5}$
0.5	0.2493527	0.2493911	$3.8e^{-5}$

A second simulation was run with a common coefficient of restitution of $e = 1$ and with the first *two* spheres released so that they strike the third with a speed v_1 (see Figure 2.13). Theoretically, the fourth and fifth spheres are both imparted a speed of v_1 , thus conserving both momentum and energy. A VISUAL NASTRAN file named *NewtonCradle2.wm3* shows that the energy is conserved to within $5.0e^{-5}$ and the ensuing motion is correctly rendered.

²Mechanical designs should not be predicated on collision solutions which arise from using impulse-momentum theory and a coefficient of restitution. This theory is a gross *approximation* to the actual collision event.

³The VISUAL NASTRAN results for $e \geq 0.5$ are substantially more accurate than those for $e < 0.5$.

Bibliography

- [1] Beer, F.P., and Johnston, R.Jr., *Vector Mechanics for Engineers: Statics, 6th ed.*, McGraw-Hill Companies, Inc., New York, NY, 1996.
- [2] Fogiel, M., *The Mechanics Problem Solver*, Research and Education Association, New York NY, 1984.
- [3] Fox, L., *Numerical Solutions of Ordinary and Partial Differential Equations*, Addison-Wesley, Palo Alto, 1962.
- [4] Hart, D., and Croft, T., *Modelling with Projectiles*, Ellis Horwood Limited, Chichester, England, 1988.
- [5] Den Hartog, J. P., *Mechanics*, Dover Publications Inc., New York, 1948.
- [6] Hughes, P. C., *Spacecraft Attitude Dynamics*, John Wiley & Sons, New York, 1986.
- [7] Inman, D. J., *Engineering Vibration*, Prentice Hall, New Jersey, 1994.
- [8] Kane, T.R., and Levinson, D.A., “An explicit solution of the general two-body collision problem”, *Computational Mechanics*, Vol. 2, 1987, pp. 75-87.
- [9] Kane, T.R., “Mechanical Demonstration of Mathematical Stability and Instability”, *International Journal of Engineering Education* or *Journal of Mechanical Engineering Education*, Vol. 2, No. 4, 1974, pp. 45-47.
- [10] Kane, T.R., and Levinson, D.A., *Dynamics: Theory and Applications*, McGraw-Hill, New York, 1985.
- [11] Meriam, J.L. and Kraige, L.G., *Engineering Mechanics: Dynamics, Vol 2., 2nd ed.*, John Wiley and Sons, Inc., New York, NY, 1987.
- [12] Meirovitch, L., *Analytical Methods in Vibrations*, Macmillan Publishing Co., New York, 1967.
- [13] Mitiguy, P.C., “Efficient Formation and Solution of Equations of Motions” *Ph.D. Thesis*, Stanford University, Department of Mechanical Engineering, 1995.
- [14] Banerjee, A.K., and Mitiguy, P.C., “Unified Computation of Stick-Slide Friction: Application to Rattlebacks, Tops, and Journal Bearings,” *Proceedings of AIAA Guidance, Navigation, and Controls Conference*, Paper 95-3350, Aug. 7-10 1995, pp. 1616-1622.

- [15] Reckdahl, K.J., "Dynamics and Control of Mechanical Systems Containing Closed Kinematic Chains" *Ph.D. Thesis*, Stanford University, Department of Mechanical Engineering, 1997.
- [16] Riley,W. and Sturges,L., *Engineering Mechanics:Dynamics*, John Wiley and Sons, Inc., New York, NY, 1993.
- [17] Serway, R., *Physics: For Scientist and Engineers with Modern Physics, 3rd ed.*, Saunders College Publishing, San Francisco, CA, 1990.
- [18] Schiehlen, W., *Multibody System Handbook*, Springer-Verlag, Berlin,Germany, 1990.
- [19] Schaechter, D.B., and Levinson, D.A., "Interactive Computerized Symbolic Dynamics for the Dynamicist," *The Journal of the Astronautical Sciences*, Vol. 36, No. 4, October-December 1988, pp. 365-388.
- [20] Soong, T., "The Dynamics of Javelin Throw," *Journal of the Applied Mechanics*, June 1975, pp. 257-262.
- [21] Synge, J. L., Griffith, B.A., *Principles of Mechanics*, McGraw-Hill Book Co. Inc., 1949.